PULMONARY TEXTURES CLASSIFICATION USING A DEEP NEURAL NETWORK WITH APPEARANCE AND GEOMETRY CUES

Rui Xu[1,2] Zhen Cong[1,2] Xinchen Ye[1,2*] Yasushi Hirano[3] Shoji Kido[3]

[1]DUT-RU International School of Information Science & Engineering, Dalian University of Technology, China
[2]Key Laboratory for Ubiquitous Network and Service Software of Liaoning Province, China
[3]Graduate School of Science and Technology for Innovation, Yamaguchi University, Japan
*Email: yexch@dlut.edu.cn

Introduction

Classification of pulmonary textures on CT images is essential for the development of CAD system of diffuse lung diseases, which usually exhibit several kinds of opacities that are widely distributed inside lungs on CT images. Fig. 1 is an example of normal lungs and lungs with severe lung diseases.

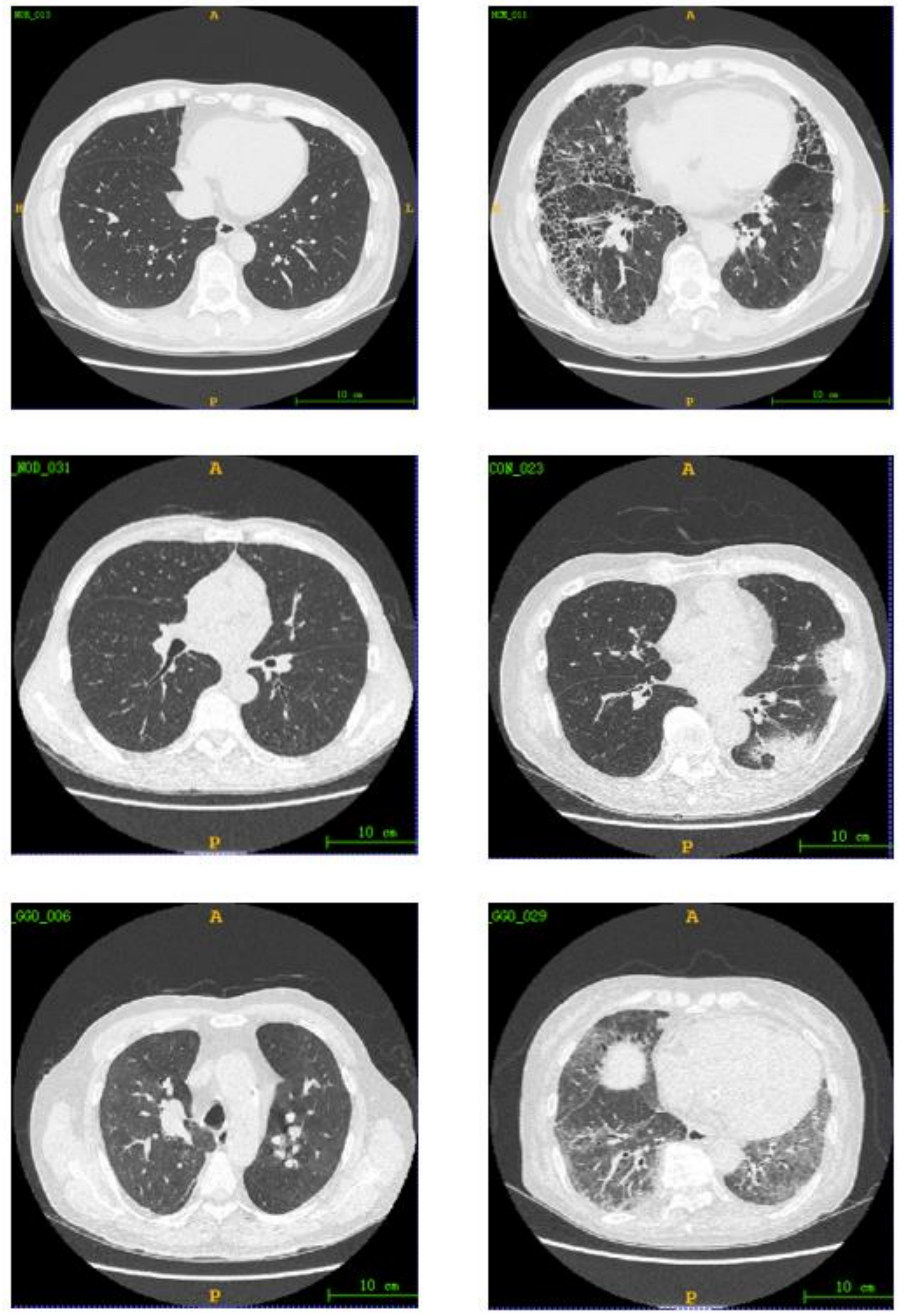

Fig. 1 Examples of CT image of normal lungs (top-left) and severe lung diseases (others)

However, the variations of textures in both global appearance and local structures with specific geometry make it difficult to achieve a high accuracy in classification task.

Recently, deep networks have had a big impact in many fields of computer vision, which include image classification. Many methods have been proposed to classify pulmonary textures by using convolutional neural networks, but the results of these methods are still not satisfying for the requirement of practical CAD system.

In this work, we propose and evaluate a deep neural network with dual-branch to classify seven kinds of pulmonary textures in CT images of diffuse lung diseases. The proposed method can achieve a better classification result comparing with state-of-the-art methods.

Deep Neural Network with Dual-branch

Normal deep convolutional neural network which is composed of several convolutional layers to compute features and fully connected layers to learn a classifier has two shortcomings. The first one is the shallow of architecture, which is a impediment of exploiting underlying information from data, and the second one is the lack of taking advantage of geometry information, as some various kinds of textures are similar in appearance but different in geometry.

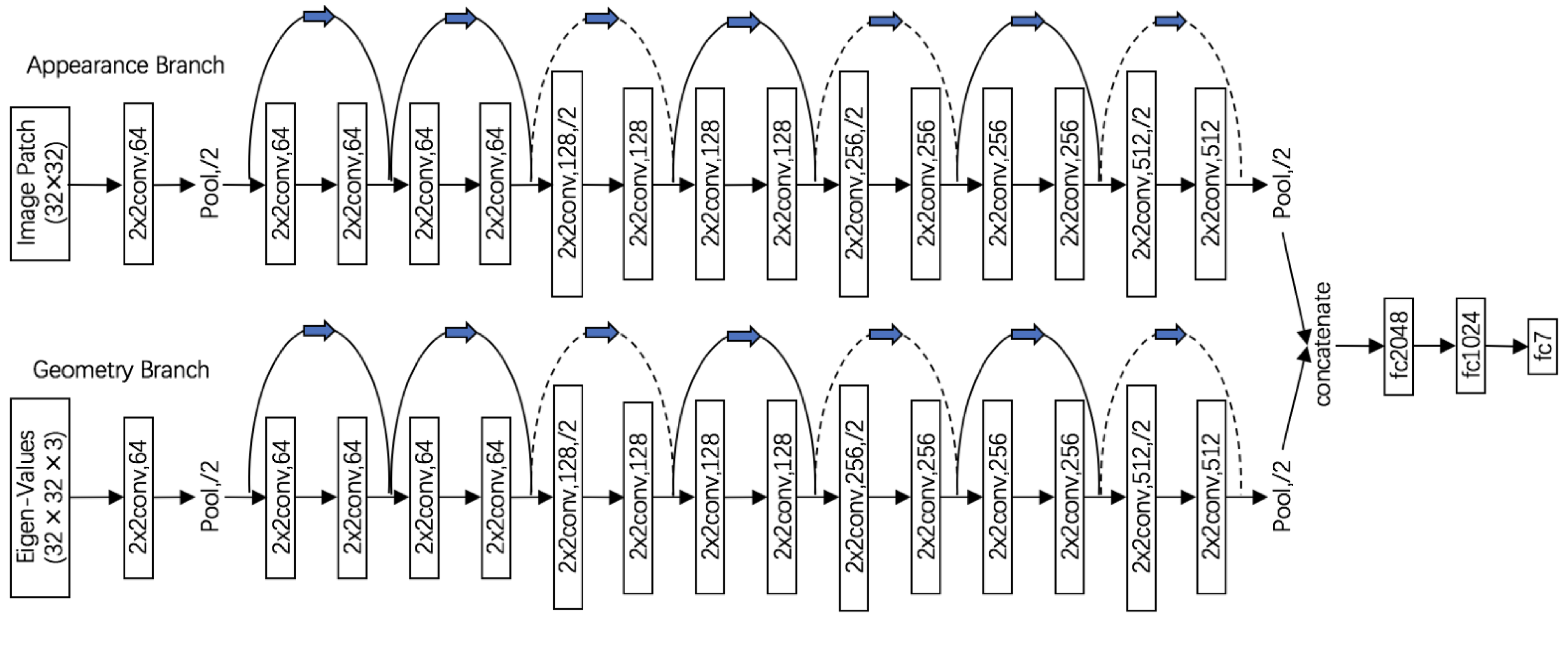

Fig. 2 The architecture of the deep neural network with dual-branch

Fig. 2 shows the architecture of the deep neural network with dual-branch, the input of lower branch is equipped with eigen-values.

The eigen-values corresponding to CT images are calculated by Hessian matrices, which is described as Eq. 1.

$$\mathbf{H}(x,y,z) = \begin{pmatrix} \frac{\partial^2 I}{\partial x^2} & \frac{\partial^2 I}{\partial x \partial y} & \frac{\partial^2 I}{\partial x \partial z} \\ \frac{\partial^2 I}{\partial y \partial x} & \frac{\partial^2 I}{\partial y^2} & \frac{\partial^2 I}{\partial y \partial z} \\ \frac{\partial^2 I}{\partial z \partial x} & \frac{\partial^2 I}{\partial z \partial y} & \frac{\partial^2 I}{\partial z^2} \end{pmatrix} \quad (1)$$

For detail, $I(x,y,z)$ is the CT intensity at a pixel on CT image patch (32 x 32 x 1). The 3 x 3 Hessian matrices are calculated on every pixel of CT image patches. By decomposing these matrices, three eigen-values can be calculated. These values are reformed to a 32 x 32 x 3 cubic, which is rich for geometry information and is utilized as the input of lower branch.

Experimental Results

Our work uses a dataset which consists of seven categories of typical pulmonary textures on CT images. They are consolidation (CON), honeycombing (HCM), nodular opacity (NOD), emphysema (EMP), multi-focal ground-glass opacity (M-GGO), reticular ground-glass opacity (R-GGO) and normal pulmonary tissues (NOR), which are shown in Fig 3.

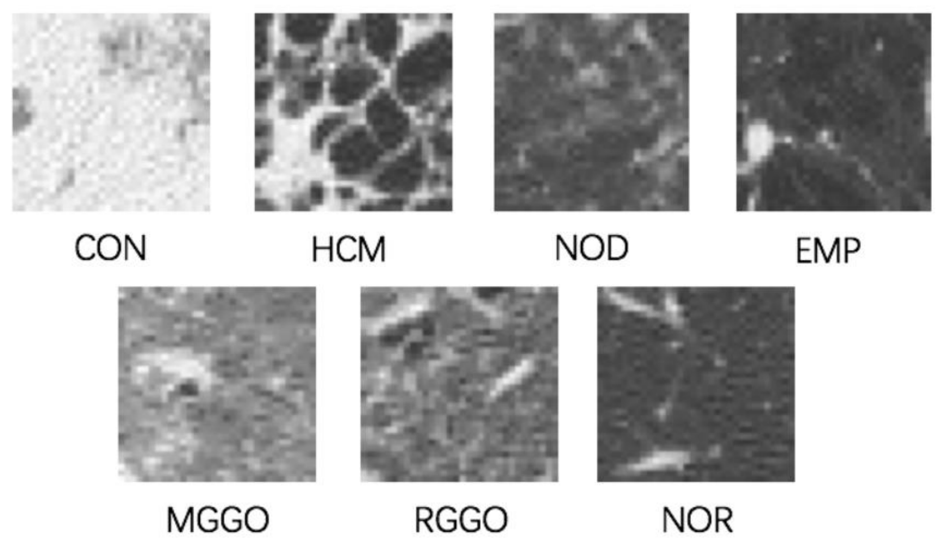

Fig. 3 Examples of pulmonary textures on CT images

Table. 1 shows the classification performance of different methods, which are the LeNet, bag-of-features based method, the CNN-based method (CNN-8), residual network (ResNet-18) and the proposed dual-branch deep network (DB-ResNet-18). We use accuracy and F-value to evaluate model's performance. Accuracy is defined as the ratio of the number of correctly classified samples and the total number of testing samples. F-value is defined as Eq. 2. We can get from the table that the proposed method outperforms all competitors.

Methods	Accuracy	F_{avg}
LeNet	0.7897	0.7921
Bag-of-Features	0.9014	0.9003
CNN-8	0.9025	0.9039
ResNet-18	0.9247	0.9247
DB-ResNet-18 (proposed)	**0.9367**	**0.9365**

Table. 1 Comparison of performances of different methods

$$F_{avg} = \frac{2}{7}\sum_{c=1}^{7}\frac{r_c \times p_c}{r_c + p_c} \quad (2)$$

$$r_c = \frac{\text{number of samples correctly classified as } c}{\text{number of samples in class } c}$$

$$p_c = \frac{\text{number of samples correctly classified as } c}{\text{number of samples classified class } c}$$

Table. 2 shows detail confusion matrices of the above methods. By comparing r_c and p_c of each category, we can directly find that the proposed method outperforms all other competitors.

	CON	MGGO	HCM	RGGO	EMP	NOD	NOR	r_c
CON	1812	3	1	55	0	3	3	0.965
MGGO	140	2244	2	144	5	10	12	0.878
HCM	0	3	2594	133	0	0	0	0.950
RGGO	112	332	92	1804	0	15	0	0.766
EMP	0	0	12	0	2402	20	16	0.980
NOD	1	23	0	2	0	2200	567	0.788
NOR	0	4	0	2	0	58	3130	0.980
p_c	0.877	0.860	0.960	0.843	0.998	0.954	0.840	

(a) Bag-of-Features

	CON	MGGO	HCM	RGGO	EMP	NOD	NOR	r_c
CON	1876	0	0	1	0	0	0	0.999
MGGO	16	2188	10	214	13	103	13	0.856
HCM	0	1	2674	55	0	0	0	0.979
RGGO	6	463	111	1775	0	0	0	0.754
EMP	0	17	48	0	2198	21	166	0.897
NOD	0	117	0	0	5	2471	200	0.885
NOR	0	65	0	0	21	84	3024	0.947
p_c	0.988	0.767	0.941	0.868	0.983	0.922	0.889	

(b) CNN-8

	CON	MGGO	HCM	RGGO	EMP	NOD	NOR	r_c
CON	1877	0	0	0	0	0	0	1.000
MGGO	22	2006	10	336	34	133	16	0.785
HCM	0	8	2634	88	0	0	0	0.965
RGGO	25	190	97	2043	0	0	0	0.868
EMP	0	0	1	0	2404	17	28	0.981
NOD	0	15	0	0	18	2509	251	0.898
NOR	0	9	0	0	8	47	3130	0.980
p_c	0.976	0.900	0.961	0.828	0.976	0.927	0.914	

(c) ResNet-18

	CON	MGGO	HCM	RGGO	EMP	NOD	NOR	r_c
CON	1868	0	0	0	3	6	0	0.995
MGGO	23	2069	2	324	56	68	15	0.809
HCM	0	0	2662	68	0	0	0	0.975
RGGO	9	128	81	2137	0	0	0	0.907
EMP	1	2	38	0	2367	8	34	0.966
NOD	0	36	0	0	7	2560	190	0.917
NOR	0	16	0	0	10	12	3156	0.988
p_c	0.983	0.919	0.957	0.845	0.969	0.965	0.930	

(d) DB-ResNet-18

Table. 2 Confusion matrices of different methods

Conclusion

We proposed a novel method to classify pulmonary textures by utilizing a deep network with a dual-branch architecture, which favors exploiting underlying information of both appearance and geometry on pulmonary textures. Experimental results showed that the proposed method outperformed four methods, including two state-of-the-art methods.